Curve-to-Image Based Non-Rigid Registration of Digital Photos and Quantitative Light-Induced Fluorescence Images in Dentistry

Benjamin Berkels[1], Thomas M. Deserno[2], Eva E. Ehrlich[3], Ulrike B. Fritz[3], Ekaterina Sirazitdinova[2], Rosalia Tatano[1]

[1]AICES Graduate School, RWTH Aachen University
[2]Department of Medical Informatics, Uniklinik-RWTH Aachen University
[3]Department of Orthodontics, Uniklinik-RWTH Aachen University
tatano@aices.rwth-aachen.de

Abstract. Decalcification is an undesirable effect that can arise during orthodontic treatment. In digital photographs, it appears as white spot lesions, i.e. white spots on the tooth surface. To asses the extent of demineralization in a tooth, quantitative light-induced fluorescence (QLF) is used. We propose a method to match digital photographs and QLF images of decalcified teeth, based on the idea of curve-to-image matching. It extracts a curve representing the shape of the tooth from the QLF image and aligns it to the photo. The registration problem is formulated as minimization problem where the objective functional consists of a data term and a higher order, linear elastic prior for the deformation. The data term is constructed using the signed distance function of the tooth region shown in the photo, which is determined in a pre-processing step by classifying the photo into tooth and non-tooth regions. The resulting minimization problem is reformulated as a nonlinear least-square problem and solved numerically using Gauss-Newton. The evaluation is based on 150 image pairs captured from 32 patients. The correctness of the matching is confirmed by visual inspection of dental experts and the alignment improvement quantified using mutual information. The curve-to-image matching idea can be extended to surface-to-voxel tasks.

1 Introduction

The mineral loss on a tooth due to plaque accumulation is termed demineralization. It is an undesirable side effect of orthodontic treatment, for example, when wearing braces [1]. Decalcification of the hard tooth tissue, a frequent form of demineralization, appears visually as white spot lesion (WSL) [2]. WSLs are considered to be a preliminary stage of incipient caries (initial lesion). In digital photography, a WSL is depicted as chalky-white, opaque enamel areas [3].

Quantitative light-induced fluorescence (QLF) is a valuable tool to asses demineralization qualitatively as well as quantitatively [4]. In QLF, demineralization is shown as dark area on the tooth surface. The outcome of the two modalities for the detection of initial caries lesions has been compared by Heinrich-Weltzien et

T. Tolxdorff et al. (Hrsg.), *Bildverarbeitung für die Medizin 2016*,
DOI 10.1007/978-3-662-49465-3_16,

al. [5] in an in-vivo clinical study. However, a disagreement between the presence and location of potential lesions is often reported.

In this paper, a multi-modal image registration approach is proposed to superimpose digital photography and QLF. Our approach is based on the idea of curve-to-image matching [6]. Compared to our previous paper [6], we introduce an improved curve extraction method that gives better control of the curve regularity.

2 Method

To register a QLF image and a photo of a tooth, a curve representing the tooth shape is extracted from the QLF image and then aligned to tooth area shown in the photo. Since the two modalities are acquired manually with different devices, the images have slightly different view angles. The resulting shape deviations are compensated with a non-rigid registration model. The proposed curve-to-image registration method is also used for the extraction of the curve from the QLF image by aligning a circle to the tooth area shown in the QLF.

2.1 Pre-processing

For registration and curve extraction, photography and QLF image are classified into tooth and non-tooth regions. To this end, the corresponding color input image is first converted to grayscale, segmented, and thresholded, where the initial grayscale conversion is adapted to the imaging modality.

The three-channel QLF image is converted to grayscale using the transformation $Y_{\mathrm{QLF}} = 0.2125R_{\mathrm{QLF}} + 0.7154G_{\mathrm{QLF}} + 0.0721B_{\mathrm{QLF}}$. Here, the weights are from the ITU-BT.709 standard for digital color encoding, while R_{QLF}, G_{QLF} and B_{QLF} denote the red, green and blue components of the QLF image.

Visually, the white color of the tooth and the color of the gingiva cannot be distinguished easily. To enhance the contrast in red, green, and blue (RGB) photography, the color space is transformed to (YC_bC_r) using

$$Y = w_R R + (1 - w_B - w_R)G + w_B B,\ C_b = \tfrac{0.5}{1-w_B}(B - Y),\ C_r = \tfrac{0.5}{1-w_R}(R - Y)$$

where $w_R = 0.299$, $w_B = 0.114$ and $w_C = 0.587$, while Y denotes the luminance component, and C_b and C_r are the blue-difference and red-difference chroma components, respectively. The YC_bC_r image is then converted to a single channel image by multiplying the components via $f_{\mathrm{prod}} = Y(1 - C_b)(1 - C_r)$ (Fig. 1).

The two resulting single-channel images are further processed using a multiphase Mumford-Shah segmentation approach [7] (three phases for the QLF image and four phases for the digital photo) and thresholded using the intensity values of these regions in such a way that the points of the two regions with higher intensity values are put into the subregion of the image where teeth are visible, named S, and the points of the other regions into the complement of S.

2.2 Modeling

Variational approach Let $\mathcal{C}$ be a curve representing the outline of the tooth extracted from the QLF image. The curve is given as a set of N points $\mathcal{C} = \{(x_i, y_i)\}_{i=1}^N = \{c_i\}_{i=1}^N$. Let $S \subset \Omega := [0,1]^2$ be the subregion of the photographic image where teeth are visible, d denotes the signed distance function of S, i.e., $d(c, S) = \pm\text{dist}(c, \partial S)$ is the Euclidean distance of the point c to the boundary of S. The sign is positive if c is outside of S and negative otherwise.

The goal of the registration is to align the curve $\mathcal{C}$ to the boundary of the tooth set S with a non-rigid deformation $\phi : \Omega \to \mathbb{R}^2$. The deformation ϕ is expressed in terms of a displacement $u = (u_1, u_2) : \Omega \to \mathbb{R}^2$ via $\phi(x) = x + u(x)$ for $x \in \Omega$. The alignment is achieved by minimizing the energy

$$E[u] = E_{\text{match}}[u] + E_{\text{reg}}[u] = \frac{1}{2}\sum_{i=1}^{N} w_i \left(d(c_i + u(c_i), S)\right)^2 + \frac{\lambda^2}{2}\int_\Omega \|\Delta u(x)\|^2 \mathrm{d}x$$

The data term $E_{\text{match}}[u]$ estimates the mismatch between the curve and the boundary of the tooth set. Furthermore, $\lambda > 0$ is a parameter that controls the smoothness of u. Although the data term only involves the displacement of the curve points, the higher order regularizer extends the displacement to the whole photo domain. Thus, the entire photo is aligned to the QLF image with $f \circ \phi$. The weights $w_i > 0$ are defined as $w_i = \left|\left(\frac{\boldsymbol{v}_i}{|\boldsymbol{v}_i|}\right)_x\right|$, where $\boldsymbol{v}_i = \frac{1}{2}(c_{i+1} - c_i) + \frac{1}{2}(c_i - c_{i-1}) = \frac{1}{2}(c_{i+1} - c_{i-1})$, which characterizes the orientation of the curve. This choice is due to the fact that neighboring teeth cannot be separated clearly (Fig. 1). Usually, the vertical boundary in S is missing, which hampers the matching of curve points in that area. The weights handle this issue since the more vertical the curve is at c_i, the smaller w_i.

Discretization and minimization A bilinear finite element (FE) discretization on a uniform rectangular grid of the image domain Ω is applied to solve the minimization problem numerically. Even though the regularizer involves second derivatives, it can be approximated with bilinear elements via $E_{\text{reg}}[u] = \frac{\lambda^2}{2}\sum_{i=1}^{2} \|M^{\frac{1}{2}} L U_i\|^2$, where M is the lumped mass matrix and L the stiffness matrix [8]. Here, U_i is the vector of nodal values that uniquely represents the FE function u_i. Using the previous approximation for the regularizer and defining the vector $F[u] = \left[\{\sqrt{w_i} d(c_i + u(c_i))\}_{i=1,\dots,N}, \lambda M^{-\frac{1}{2}} L U_1, \lambda M^{-\frac{1}{2}} L U_2\right]^T$, the

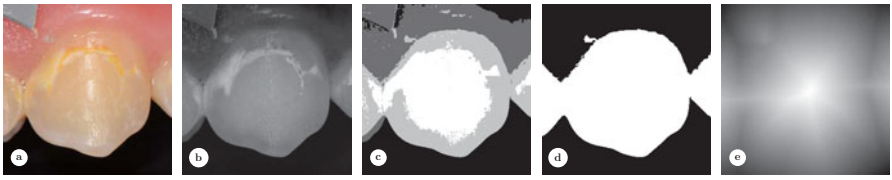

Fig. 1. Image processing: (a) Photo, (b) product image f_{prod}, (c) segmentation, (d) tooth region S_f and (e) signed distance function d of S_f.

minimization problem can be reformulated as a nonlinear least square problem via $E[u] = \frac{1}{2}\|F[u]\|^2$ and solved using Gauss-Newton [9]. To provide a good initial guess for the minimization, a regularized affine registration is performed [10]. It is based on the same data term as the non-rigid model and the Dirichlet energy as prior for the deformation, since the Laplacian of an affine deformation vanishes. The affine deformation ϕ is defined as $\phi(c) = Ac + t$, where A is 2×2 matrix and t a translation vector. The non-rigid problem is solved successively for decreasing values of λ to achieve a coarse-to-fine matching, which helps the minimization not to get stuck in local minima.

Curve extraction The curve $\mathcal{C}$ is extracted from the QLF image by applying the algorithm just described to register a suitable curve to the QLF image. First (Sect. 2.1), a classification of the QLF image into tooth and non-tooth regions is performed to get the set S_{QLF} (tooth region of the QLF image). Since a tooth is topologically equivalent to a circle, we chose $\mathcal{C}$ as a small circle in the center of the QLF image, and apply the registration algorithm to $\mathcal{C}$ and S_{QLF}. The circle is deformed iteratively to align with the boundary of S_{QLF} yielding the shape of the tooth (Fig. 2).

2.3 Data and evaluation

Data acquisition All photos were acquired with a digital SLR (Nikon D7000, Japan) under standardized conditions, using a macro lens (Nikkor 105 mm, 1: 2.8) with a ring flash (Sigma EM-140 DG). The QLF images were recorded using the InspektorPro system (Panasonic WV-KS 152 QLF|clin, QLF software version 2.0.0.49, Inspector Research System BV, The Netherlands). A total of 150 QLF/photo image pairs were acquired from 32 subjects after brace removal.

Evaluation The accuracy of the proposed registration method was qualitatively confirmed by visual inspection of medical experts. Since no ground truth was available, the alignment improvement by the registration is quantified using the mutual information (MI) of the QLF images and of the digital photographs.

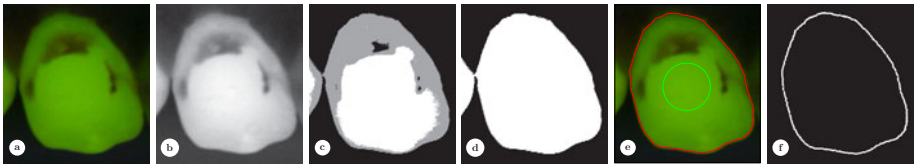

Fig. 2. Curve extraction: (a) QLF image, (b) grayscale QLF image, (c) segmented grayscale image, (d) tooth region S_{QLF}, (e) QLF with the initial circle (green) and curve after the non-rigid registration (red), and (f) final curve $\mathcal{C}$.

3 Results

The parameters for the curve extraction are obtained empirically and set to $\lambda = 0.1$ and $\lambda = 10^{-i},\ i = \{2, 3, 4\}$ for the parametric registration step and the non-rigid step, respectively. To match QLF and photographs, $\lambda = 1$ and $\lambda = 10^{-i},\ i = \{1, 2, 3, 4\}$ were used. Similar results are obtained in 139 out of 150 cases (Fig. 3). In the 11 problematic cases, the extracted QLF curve was inaccurate. Figure 4 shows five of these cases.

For all 150 image pairs, the MI value decreases after the registration. The mean MI value of all image pairs is -2962.80 ± 529.436 before and -3884.53 ± 585.817 after the registration. A two-tailed t-test revealed that the difference in the mean MI values before and after the registration statistically is significant at the 5% level (p-value < 0.0001).

4 Discussion

A novel method for the registration of photographs and QLF images of human teeth is proposed. The method is based on curve-to-image matching and successfully applied to clinical images. The proposed registration method is used to assess the relation between decalcification as shown by QLF and digital photography. For all 150 pairs of images, three medical experts marked the decalcified areas of the teeth. By aligning the QLF image and the digital photograph using the proposed method, it is possible to compare the marked decalcified areas and quantitatively assess the overlap using the Dice coefficient. Similarly,

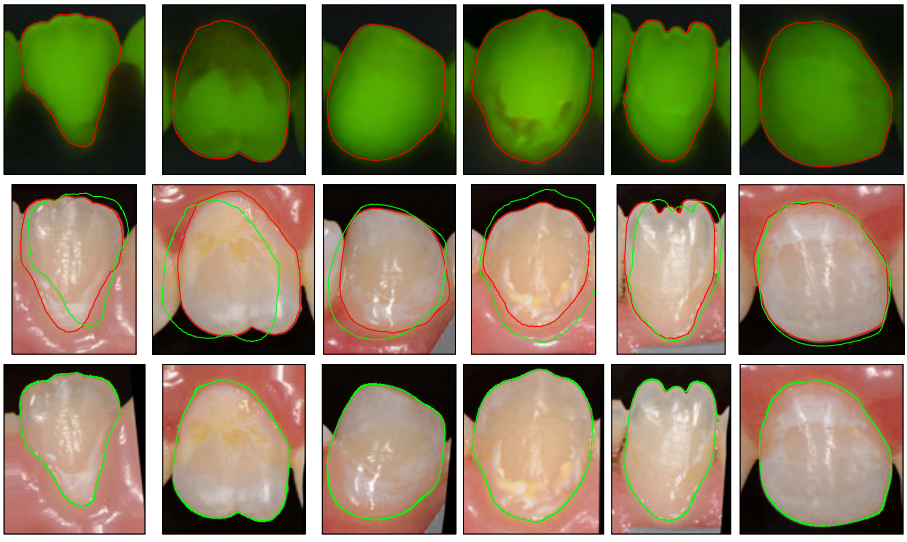

Fig. 3. Results for six image pairs: QLF image with segmented curve (red), photo with the initial QLF curve (green) and curve after the non-rigid registration (red) and deformed photo with the QLF curve (green).

Fig. 4. Five cases detected by visual inspection where the curve extraction fails.

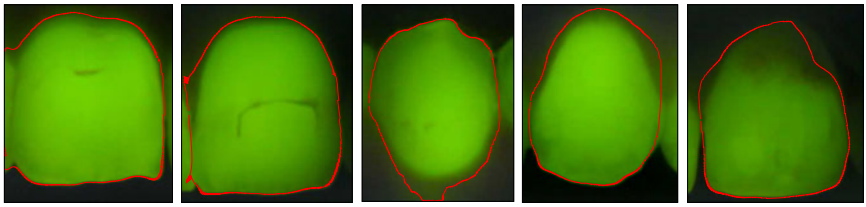

the intra-rater and inter-rater reliability can be evaluated. Our study indicates that the agreement between QLF and photography is much lower than inter- and intra-observer variability, which indicates that QLF and photography show complementary information about the damage.

The proposed curve-to-image matching can be extended to surface-to-voxel matching. The same ideas can be used for multimodal 3D registration problems, for instance, to register a volumetric patient scan to a segmented atlas. In this case, the role of the curve is taken by the boundary surfaces of the atlas segments, while the volumetric patient scan replaces the photograph.

References

1. Ousehal L, Lazrak L, Es-Said R, et al. Evaluation of dental plaque control in patients wearing fixed orthodontic appliances: a clinical study. Int Orthod. 2011;9:140–55.
2. Palamara J, Phakey PP, Rachinger WA, et al. Ultrastructure of the intact surface zone of white spot and brown spot carious lesions in human enamel. J Oral Pathol. 1986;15(1):28–35.
3. Gorelick L, Geiger AM, Gwinnett AJ. Incidence of white spot formation after bonding and banding. Am J Orthod. 1982;81(2):93–8.
4. Srivastava K, Tikku T, Khanna R, et al. Risk factors and management of white spot lesions in orthodontics. J Orthod Sci. 2013;2(2):43–9.
5. Heinrich-Weltzien R, Kühnisch J, Ifland A, et al. Detection of initial caries lesions on smooth surfaces by quantitative light-induced fluorescence and visual examination: an in vivo comparison. Eur J Oral Sci. 2005;113(6):494–8.
6. Berkels B, Deserno TM, Ehrlich EE, et al. Non-rigid contour-to-pixel registration of photographic and quantitative light-induced fluorescence imaging of decalcified teeth. SPIE Med Imaging. 2016;Accepted.
7. Zach C, Gallup D, Frahm JM, et al. Fast global labeling for real-time stereo using multiple plane sweeps. Proc Int Fall Workshop Vis Model Vis. 2008; p. 243–52.
8. Berkels B, Cabrillo I, Haller S, et al. Co-registration of intra-operative photographs and pre-operative MR images. Int J Comput Assist Radiol Surg. 2014;9(3):387–400.
9. Gratton S, Lawless AS, Nichols NK. Approximate gauss-newton methods for non-linear least squares problems. SIAM J Optim. 2007;18(1):106–32.
10. Chumchob N, Chen K. A robust affine image registration method. Int J Num Anal Model. 2009;6(2):311–34.